Cytotechnology (2013) 65:447–455
DOI 10.1007/s10616-012-9499-1

ORIGINAL RESEARCH

Galangin induces B16F10 melanoma cell apoptosis via mitochondrial pathway and sustained activation of p38 MAPK

Wenjing Zhang · Yan Lan · Qilai Huang · Zichun Hua

Received: 21 May 2012 / Accepted: 7 September 2012 / Published online: 22 September 2012

Abstract Galangin, an active flavonoid present at high concentration in Alpinia officinarum Hance and propolis, shows cytotoxicity towards several cancer cell lines, including melanoma. However, the specific cellular targets of galangin-induced cytotoxicity in melanoma are still unknown. Here, we investigated the effects of galangin in B16F10 melanoma cells and explored the possible molecular mechanisms. Galangin significantly decreased cell viability of B16F10 cells, and also induced cell apoptosis shown by Hoechst 33342 staining and Annexin V-PI double staining flow cytometric assay. Furthermore, upon galangin treatment, disruption of mitochondrial membrane potential was observed by JC-1 staining. Western blotting analysis indicated that galangin activated apoptosis signaling cascades by cleavage of procaspase-9, procaspase-3 and PARP in B16F10 cells. Moreover, galangin significantly induced activation of phosphor-p38 MAPK in a time and dose dependent manner. SB203580, an inhibitor of p38, partially attenuated galangin-induced apoptosis in B16F10 cells. Taken together, this work suggests that galangin has the potential to be a promising agent for melanoma treatment and may be further evaluated as a chemotherapeutic agent.

Keywords Galangin · Apoptosis · Malignant melanoma · Mitochondria · p38 MAPK

W. Zhang · Q. Huang · Z. Hua
The State Key Laboratory of Quality Research in Chinese Medicine, Faculty of Chinese Medicine, Macau University of Science and Technology, Taipa Macau, China

W. Zhang · Q. Huang · Z. Hua
Macau Institute for Applied Research in Medicine, Macau University of Science and Technology, Taipa Macau, China

Y. Lan · Q. Huang (✉) · Z. Hua (✉)
The State Key Laboratory of Pharmaceutical Biotechnology, Nanjing University, 210093 Nanjing, China
e-mail: biocentury@gmail.com

Z. Hua
e-mail: zchua@nju.edu.cn

Z. Hua
Changzhou High-Tech Research Institute of Nanjing University, 213164 Changzhou, China

Introduction

Malignant melanoma is becoming a major health threat as the incidence continues to rise (Ratheesh et al. 2007). The best response rate produced by a single-agent chemotherapy or biotherapy for melanoma is only 16 % (Atallah and Flaherty 2005; Chen et al. 2010). Comprehensive understanding of the molecular signaling events implicated in melanoma development and progression would offer new avenues for therapeutic intervention. Of note, the RAF/MEK/ERK mitogen-activated protein kinase (MAPK)

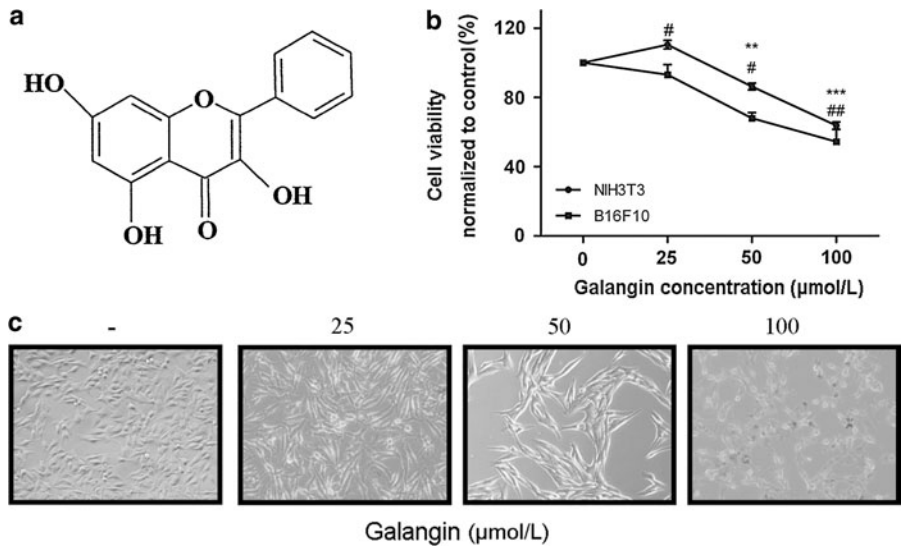

Fig. 1 Galangin inhibits B16F10 cell proliferation. **a** The chemical structure of galangin. **b** Toxicity of galangin on NIH3T3 and B16F10 cell lines. Viability was examined by the PrestoBlue™ reagent. The experiments were performed three times. Data shown represent the mean ± SEM, $\#p < 0.05$, $\#\#p < 0.01$ compared with NIH3T3 control group; $**p < 0.05$, $***p < 0.001$ compared with B16F10 control group. **c** Morphological changes of B16F10 cells induced by galangin for 24 h (magnification: ×200)

pathway is activated in most melanoma (Lopez-Bergami 2011). The MAPK family comprises extracellular signal-regulated kinase (ERK p44/42), the c-Jun N-terminal kinases (JNKs), and the p38 MAPKs. The ERK pathway activation directs cell proliferation, differentiation, and survival, whereas JNK pathway promotes either proliferation or apoptosis (Kennedy and Davis 2003). In contrast, the p38 pathway is actively responsible for cellular stress, including UV irradiation, chemotherapeutic agents, and pro-inflammatory cytokines (Han and Sun 2007).

Alpinia officinarum Hance, a traditional herbal plant, has been used as an aromatic stomachic analgesic, and antiemetic in Asia (Lu et al. 2007). Galangin (3, 5, 7-trihydroxyflavone), is found in reasonable quantities in the root of Alpinia officinarum Hance, and propolis (Fig. 1a) (Heo et al. 2001) and has been reported to possess several biological actions, such as antioxidative and radical scavenging activities (Russo et al. 2002), antimutagenic and anticlastogenic effects (Heo et al. 1996; Sohn et al. 1998). The evaluation of the toxicity of galangin has attracted much attention in recent years. In fact, anti-proliferation activity of galangin has been reported in various cancer cells, such as leukemia (Bestwick and Milne 2006), prostate cancer (Szliszka et al. 2011), breast (Murray et al. 2006), cervical and esophageal cancer (Barbaric et al. 2011; Wang et al. 2009). The mechanism of galangin-induced reduction in proliferation in mammary tumor cells was associated with targeting tumor cell cycle proteins (Murray et al. 2006). In addition, galangin showed proapoptotic potential in hepatocellular carcinoma by disrupting the mitochondrial membrane potential and translocating the pro-apoptotic protein Bax to the mitochondria, which then released apoptosis inducing factor and cytochrome C into the cytosol (Zhang et al. 2010). Research has been documented that galangin may be a whitening agent and a promising candidate for prevention of skin cancer (Lu et al. 2007; Matsuda et al. 2009). However, the detailed molecular mechanisms of galangin killing of melanoma cells remain unclear. It is also not known whether p38 MAPK is involved in the galangin-induced apoptosis in melanoma.

Indeed, we found that galangin suppressed B16F10 cell proliferation through inducing morphological changes and the appearance of apoptotic characteristics. To further explore the mechanisms of apoptosis, we demonstrated that the mitochondrial potential was disrupted and caspases were activated by galangin. Simultaneously, a gradually increased activation of p38 MAPK was observed in time and dose dependent

manners. Activation of p38 MAPK is part of the apoptotic response in B16F10 cells elicited by galangin. The results present here provide a novel insight into the molecular mechanisms underlying the cytotoxicity of galangin in B16F10 melanoma cells.

Materials and methods

Materials

Galangin was purchased from Guangzhou Institute for Drug Control (Guangzhou, China) and dissolved in dimethyl sulfoxide (DMSO) as a stock solution at 100 mmol/L. The stock solution was kept at −20 °C. P38 inhibitor SB203580 was from Cell Signaling Technology (Danvers, MA, USA) and was dissolved in DMSO as a stock solution at 10 mmol/L. Hoechst 33342 and mitochondrial membrane potential assay kit with JC-1 were from Beyotime Institute of Biotechnology (Jiangsu, China). High glucose Dulbecco's modified Eagle's medium (DMEM), fetal bovine serum (FBS), bovine calf serum, 0.05 % Trypsine-EDTA, and a penicillin–streptomycin mixture (100×) were purchased from Gibco (Invitrogen, Carlsbad, CA, USA). Primary antibodies to PARP, caspase-3, caspase-9, phosphor-p38 MAPK (Thr180/Tyr182) and p38 were from Cell Signaling Technology. Primary antibody of glyceraldehyde-3-phosphate dehydrogenase (GAPDH) was from Santa Cruz Biotechnology (Santa Cruz, CA, USA). Secondary antibodies (IRDye 800CW anti-mouse IgG and anti-rabbit IgG) were purchased from LI-COR Biosciences (Lincoln, NE, USA).

Cell culture

B16F10 cell line (murine melanoma cell) and NIH3T3 (mouse embryo fibroblast cell) cell line were purchased from American Type Cell Culture (ATCC, Manassas, VA, USA). B16F10 cells were cultured in DMEM supplemented with 10 % FBS and NIH3T3 cells were maintained in DMEM with 10 % bovine calf serum. Both media contained 100 units/mL penicillin and 100 μg/mL streptomycin. The cells were cultured under a humidified atmosphere in 5 % CO_2 at 37 °C. The cells were treated with varying concentrations of galangin with the final concentration of DMSO below 0.5 % (V/V).

Cell viability assay

Cell survival with or without galangin treatment was measured with the PrestoBlue™ reagent according to the manufacturer's protocol. Briefly, cultured B16F10 cells and NIH3T3 cells were seeded at a density of 1×10^4 cells/ml in a 96-well plate. Both cell lines were treated with 0, 25, 50, and 100 μmol/L galangin for 24 h. B16F10 cells were treated with galangin and SB203580 as a single agent or in combination for 24 h. Then cells were incubated with the PrestoBlue™ reagent for 1 h. Fluorescence intensity values were collected at $\lambda ex = 560$ nm, $\lambda em = 590$ nm with the Gemini EM Microplate Reader (Molecular Devices, Sunnyvale, CA, USA). Cell viability was calculated using the following formula: 100 % × [(fluorescence intensity of treated cells-blank group)/ (fluorescence intensity of untreated cells-blank group)].

Cell morphology observation

B16F10 cells were seeded in a 6-well plate at a density of 5×10^5 cells/well and cultured overnight. The cells were treated with 25–100 μmol/L galangin for 24 h at 37 °C in a humidified atmosphere containing 5 % CO_2. The cells were then fixed in 3.7 % paraformaldehyde and washed with PBS. The cellular morphology was visualized using a microscope (IX71, Olympus, Tokyo, Japan) and photographed.

Hoechst 33342 staining

Apoptotic nuclear features were observed by staining with Hoechst 33342. B16F10 cells were cultured in a 24-well plate and treated with 0, 25, 50, and 100 μmol/L galangin for 24 h. Then, the cells were washed with the staining buffer and incubated with 5 μL of Hoechst 33342 solution at 4 °C for 20 min. Finally, the cells were washed twice with staining buffer. The morphological features of apoptosis were observed under a fluorescence microscope (IX71, Olympus, Tokyo, Japan).

Annexin V-PI staining for flow cytometry

Cells were treated with the indicated concentrations of galangin or/and SB203580 for 24 h. B16F10 cells were labeled with FITC-conjugated-annexin V and PI (BD PharMingen) according to the manufacturer's instructions, and analyzed by flow cytometry (Becton–Dickinson,

San Jose, USA). The data were analyzed with Cell Quest software version 3.3 (Becton–Dickinson, San Jose, USA).

JC-1 staining

The mitochondrial membrane potential was assessed with the fluorescent probe JC-1 dye. Briefly, B16F10 cells were treated with galangin (0, 25, 50, and 100 μmol/L) for 12 h. Then, cells were incubated with JC-1 working solution for 20 min at 37 °C in the dark. Cells were washed with cold JC-1 staining buffer, placed on ice and observed immediately with a fluorescence microscope to record cells with JC-1 in red–orange aggregates form and cells with JC-1 in green monomeric form. The fluorescence intensity of both JC-1 monomers (λex = 490 nm, λem = 530 nm) and aggregates (λex = 525 nm, λem = 590 nm) was also collected by the Gemini EM Microplate Reader.

Western blotting

B16F10 cells were treated with galangin at the indicated concentrations (0, 25, 50, and 100 μmol/L) for 24 h and 50 μmol/L galangin for various duration (0, 2, 4, 8, 12, 16, 20, and 24 h). Cells were washed twice with cold PBS and lysed on ice for 30 min in lysis buffer (50 mmol/L Tris–HCl pH 7.5, 150 mmol/L NaCl, 1 % Triton-X 100, 0.5 % sodium deoxycholate, 0.1 % SDS, 5 mmol/L EDTA, 10 mmol/L NaF, 1 mmol/L sodium vanadate (Na_3VO_4), 10 % glycerol, and 1 mmol/L EGTA). The lysates were cleared by centrifugation at 12,000 rcf for 30 min at 4 °C and the protein concentrations were determined using the Bradford assay. For immunoblotting, lysate samples containing equal amounts of protein (30–40 μg) were submitted to electrophoresis on SDS-PAGE gels and transferred to nitrocellulose membrane. The membranes were first incubated in blocking solution (5 % nonfat milk) for 1 h and then were probed with antibodies against PARP, caspase-3, caspase-9, phosphor-p38 MAPK, p38 MAPK or GAPDH overnight at 4 °C. After washing with PBST (1 × PBS + 0.1 % Tween-20) three times (10 min/wash), the membranes were incubated with IRDye 800CW anti-mouse or anti-rabbit secondary IgG antibodies for 2 h and then washed with PBST three times (10 min/wash). Finally, fluorescence labeled protein bands were visualized by the Odyssey Infrared Imaging System (LI-COR Biosciences, Lincoln, NE, USA) using the 800 nm channel at 84 μm resolution. Signal was acquired and quantified using the Odyssey system application software (version 2.1).

Statistical analysis

The data were presented as mean ± SEM. Variance analysis between groups was performed separately by one-way ANOVA followed by Dunnett post hoc test, and a student *t* test with GraphPad Prism 5.0 software (La Jolla, CA). A p value <0.05 was considered statistically significant. Each experiment was performed independently in triplicate and similar results were obtained.

Results

Galangin suppresses B16F10 cells proliferation in vitro

B16F10 cells were incubated with various concentrations of galangin for 24 h. The results showed that low doses (10 μmol/L) of galangin compared with untreated controls elicited a minimal growth response, although not as pronounced (data not shown). Higher concentrations of galangin significantly decreased the percentage of viable cells. The inhibitory rates of galangin at 50 and 100 μmol/L on cell growth were 32.07 and 45.54 % ($p < 0.05$), respectively (Fig. 1b). The IC50 of galangin to B16F10 cells during a 24 h treatment was 145.0 μmol/L. However, galangin could also decrease cell viability of NIH3T3. The results showed that 25 μmol/L galangin compared with untreated controls elicited a significant growth response ($p < 0.05$), higher concentration suppressed cell proliferation ($p < 0.05$) (Fig. 1b). These results suggested that galangin can inhibit cell proliferation both of normal cells and tumor cells, which may be accorded to its lipophilicity (Kajiya et al. 2001; Kim et al. 2006). Microscopical analysis revealed the reduced number of cells and morphological aberrations after a 24 h treatment with galangin. 25 and 50 μmol/L galangin treated cells became elongated, flatten, and shrunk. The appearance of apoptotic cells such as cell shrinking, rounding and partial detachment was evident at a galangin concentration of 100 μmol/L (Fig. 1c).

Galangin induces apoptosis in B16F10 cells

The pro-apoptotic effect of galangin on B16F10 cells was firstly visualized by Hoechst 33324 staining. Galangin suppressed the growth of B16F10 cells as shown by decline in nuclear number (Fig. 2a). Apoptotic morphological features such as cell shrinkage and dot-shaped nuclear fragments were evident in cells exposed to 100 μmol/L of galangin. Then flow cytometry was conducted to examine the apoptosis percentage. Galangin treatment groups (50 and 100 μmol/L) showed significant increases in apoptosis compared with the control group ($p < 0.001$). The apoptotic rates in the untreated group was only 2.95 %, whereas the concentration of 25, 50, and 100 μmol/L resulted in the apoptotic rates of 2.08, 15.08, and 23.41 %, respectively (Fig. 2b).

The disruption of mitochondrial transmembrane potential by galangin

The mitochondrial dye JC-1 undergoes reversible change in fluorescence emission from red–orange to green as the mitochondrial membrane potential (MMP) decreases. As shown in Fig. 3a, B16F10 cells without galangin treatment predominantly exhibited red–orange fluorescence, indicating intact mitochondrial membrane potential. Treatment with galangin for 12 h caused a fluorescence shift from red–orange to green in a dose dependent manner. The data shown are based on normalized fluorescence intensity ratio. The ratio shifted rapidly from 0.88 (25 μmol/L galangin) to 0.65 (100 μmol/L galangin) (Fig. 3b) ($p < 0.05$). These results indicated collapse of the mitochondrial membrane potential upon galangin treatment.

Galangin induces activation of apoptotic signaling cascade

Caspases play a central role in mediating the intrinsic and the extrinsic apoptosis pathways. To elucidate the mechanism of galangin-induced apoptosis, caspases in the mitochondrial apoptotic pathway were examined at protein level. As shown in Fig. 3c, galangin decreased the level of procaspase-9 and cleaved procaspase-3 into the activated forms. The activation of caspase-3 was further confirmed by detection of the degradation of PARP, which is a marker for apoptosis and undergoes cleavage by caspase-3 during apoptosis. In galangin-treated cells, the cleavage of PARP was evident at 50 and 100 μmol/L.

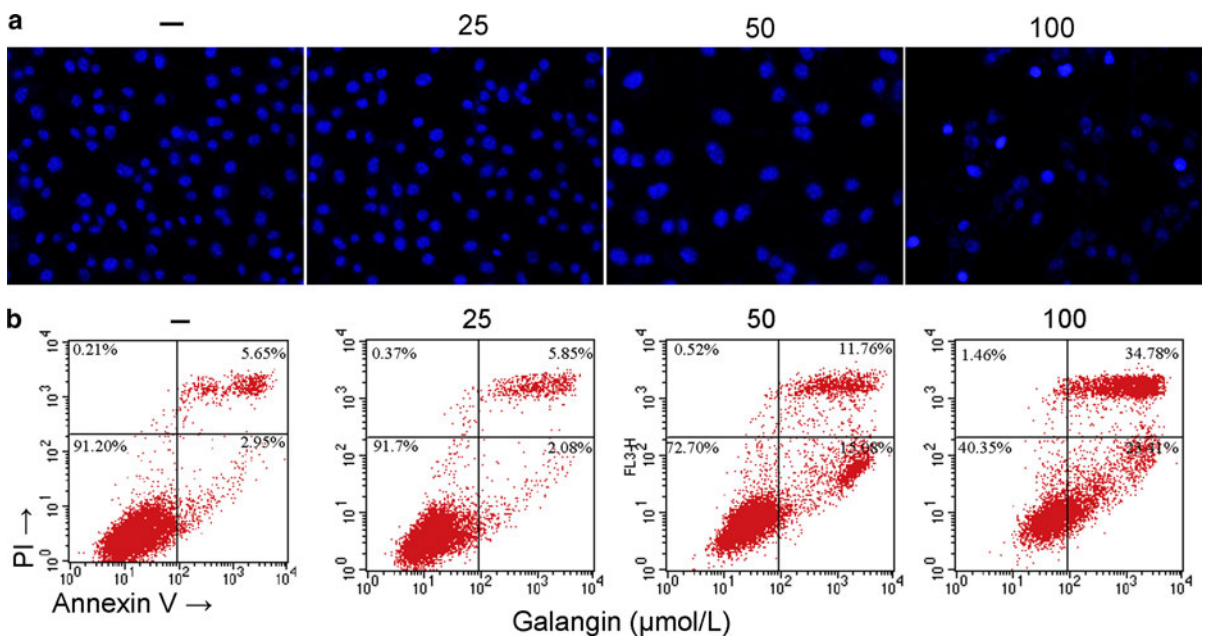

Fig. 2 Galangin elicits apoptotic cell death in B16F10 cells. **a** Representative photographs of B16F10 cells stained with Hoechst 33342 (magnification: ×400). Apoptotic cells were characterized as having condensed or fragmented nuclei. **b** Representative flow cytometric analysis of B16F10 cells stained with Annexin V-propidium iodide (PI) after treatment with 0–100 μmol/L galangin. The experiments were performed in triplicate

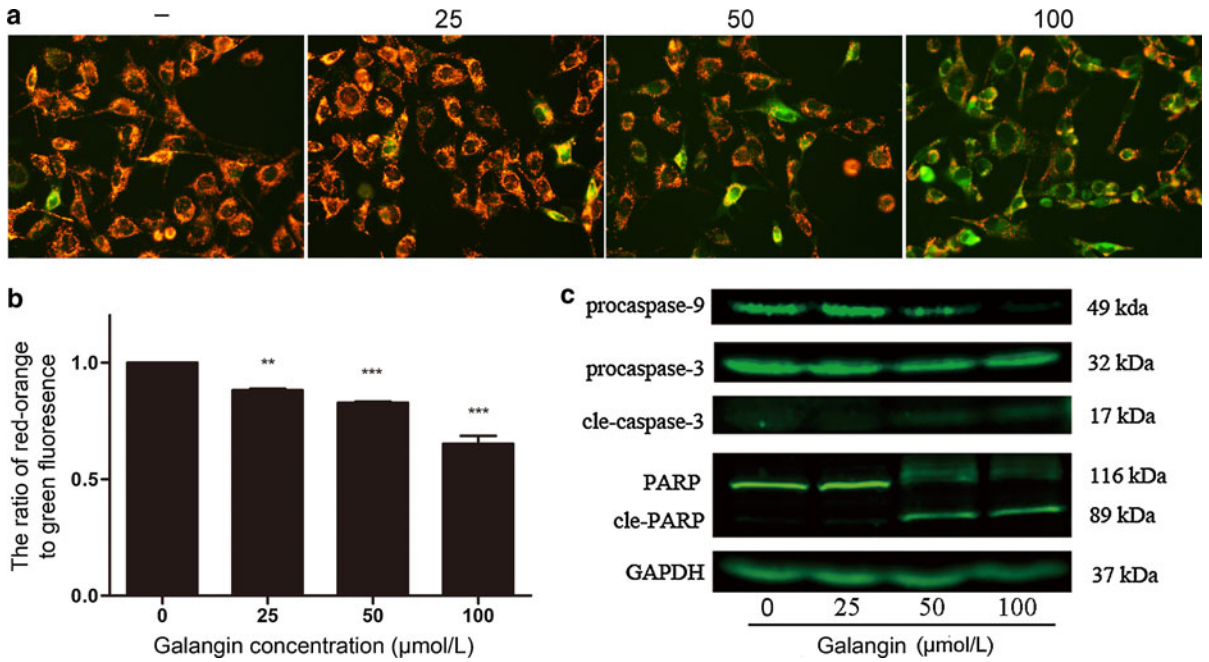

Fig. 3 Effects of galangin on mitochondrial membrane potential and apoptosis-related proteins in B16F10 cells. **a** B16F10 cells were treated with different concentrations of galangin (25–100 μmol/L) for 12 h, stained with JC-1 and observed under fluorescence microscope. Red–orange fluorescence represents mitochondria with an intact membrane potential; green fluorescence represents disrupted membrane potential (magnification: ×400). **b** Quantitative analysis of mitochondrial membrane potential by the ratio of red fluorescence intensity/green fluorescence intensity acquired with fluorescent microplate reader. Data are means ± SEM of three independent experiments. $^{**}p < 0.01$, $^{***}p < 0.001$ indicated significance compared with untreated group. **c** Representative western blots for the expression of caspase-9, caspase-3, PARP with GAPDH as an internal control. Each experiment was performed in triplicate

Galangin elicits the sustained phosphorylation of p38 MAPK

B16F10 cells were treated with 25, 50, and 100 μmol/L galangin, the level of p38 MAPK phosphorylation increased in a dose dependent manner (Fig. 4a, b); furthermore, the level of phosphor-p38 protein was examined at designed time points after treatment with 50 μmol/L galangin. The induction of phosphor-p38 MAPK was evident following galangin treatment after 2 h and increased sharply until 24 h (Fig. 4c, d).

Galangin-induced cell cytotoxicity and apoptosis are partially restored by SB203580 treatment

Because galangin seems to induce sustained activation of p38 in B16F10 cells, we used a specific p38 inhibitor, SB203580, alone or in combination with galangin to test whether galangin-induced apoptosis is mediated through the p38 MAPK signaling pathway. As shown in Fig. 5a, cell viability analyses revealed that higher concentration (≥20 μmol/L) of SB203580 alone inhibited cell proliferation compared with control group. 10 μmol/L SB203580, a concentration that has little effect on cell survival, was used in the following experiments. Cell cytotoxicity induced by 50 μmol/L galangin was moderately blocked by pretreatment with SB203580 (Fig. 5b, $p < 0.05$), however, there was no significant difference in 100 μmol/L galangin group. Flow cytometric analyses detected that SB203580 alone could induce apoptosis in B16F10 cells. Pretreatment with SB203580 reversed 50 μmol/L galangin-induced apoptosis (Fig. 5c, $p < 0.05$). Additionally, SB203580 did not protect from 100 μmol/L galangin-induced apoptotic response.

Discussion

Our results presented here showed that galangin inhibited cell viability, changed cellular morphology, and induced apotosis in B16F10 melanoma cells at

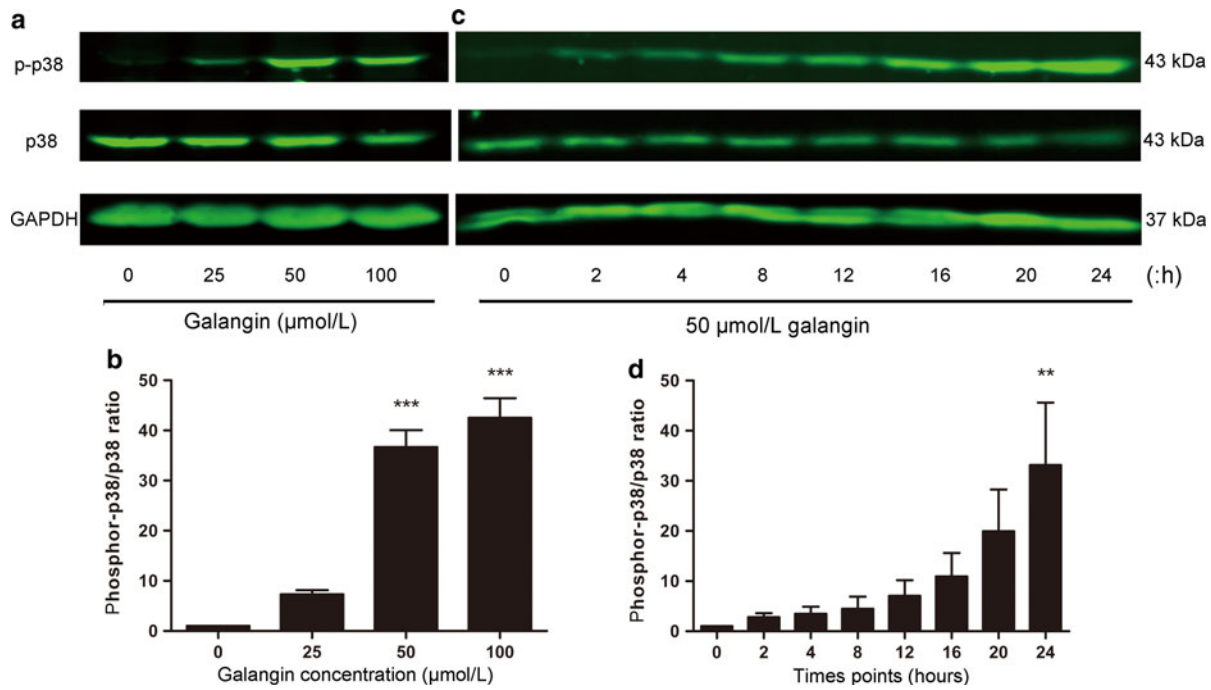

Fig. 4 Concentration- and time-dependent effects of galangin on p38 in B16F10 cells. **a** B16F10 cells were treated with 0, 25, 50 and 100 μmol/L galangin for 24 h. **c** B16F10 cells were treated with 50 μmol/L galangin for 0, 2, 4, 8, 12, 16, 20, and 24 h. Cell protein was extracted and phosphor-p38 MAPK was analyzed by western blotting. **b**, and **d** Fluorescence density of each band was quantified with the Odyssey system application software, and the ratio of phosphor-p38/p38 MAPK was calculated and normalized. The experiments were done for three times. $***p < 0.001$ versus control group; $**p < 0.01$ versus 0 h

concentrations of 50 and 100 μmol/L. Mitochondria are considered a main link between cellular stress signals and the execution of apoptotic and necrotic cell death (Gomez-Lazaro et al. 2007). Loss of mitochondrial membrane potential is an early indication in the mitochondrial mediated apoptosis. Such alternations can be observed using various dyes, based on the principle that intact and disrupted mitochondria exhibit differential patterns of dye uptake. JC-1, a membrane permeable dye, can selectively enter the mitochondria and reversibly changes color as mitochondrial membrane potential increases (Sakamuru et al. 2012). Indeed, treatment of B16F10 melanoma cells with galangin resulted in a drop of the mitochondrial membrane potential in a time and dose dependent manner. Caspases are a family of specific cysteine proteases, and their activation is critical in the intracellular execution of programmed cell death (Cohen 1997; Lavrik et al. 2005). The observation of galangin-mediated reduction of procaspase-9 and the cleavage of procaspase-3, as well as the cleavage of 116 kDa PARP into 89 kDa subunit, indicated that mitochondrial-mediated caspase cascade pathway was activated in galangin-induced apoptosis. Zhang et al. demonstrated that galangin (46.25–370.0 μmol/L) induced apoptosis by translocating the pro-apoptotic protein Bax to the mitochondrial and initiated the mitochondrial pathway in hepatocellular carcinoma cells (Zhang et al. 2010). However, we did not detect any appreciable change of Bax in B16F10 melanoma treated with galangin (25–100 μmol/L). The reasons for this discrepancy are not clear and may be due to subtle differences in the experimental systems, such as the cell type, the cellular context, or the concentrations of the stimuli.

Accumulated evidence support a tumor suppressor function of p38 MAPK in negatively regulating cell survival and proliferation (Olson and Hallahan 2004). Extensive research has documented that many chemotherapeutic agents and natural product triggered tumor cell apoptosis through activation of p38 MAPK. Betulinic acid, a selective inhibitor of human melanoma, induced apoptosis through oxidative stress-mediated p38 activation (Tan et al. 2003). Reports on

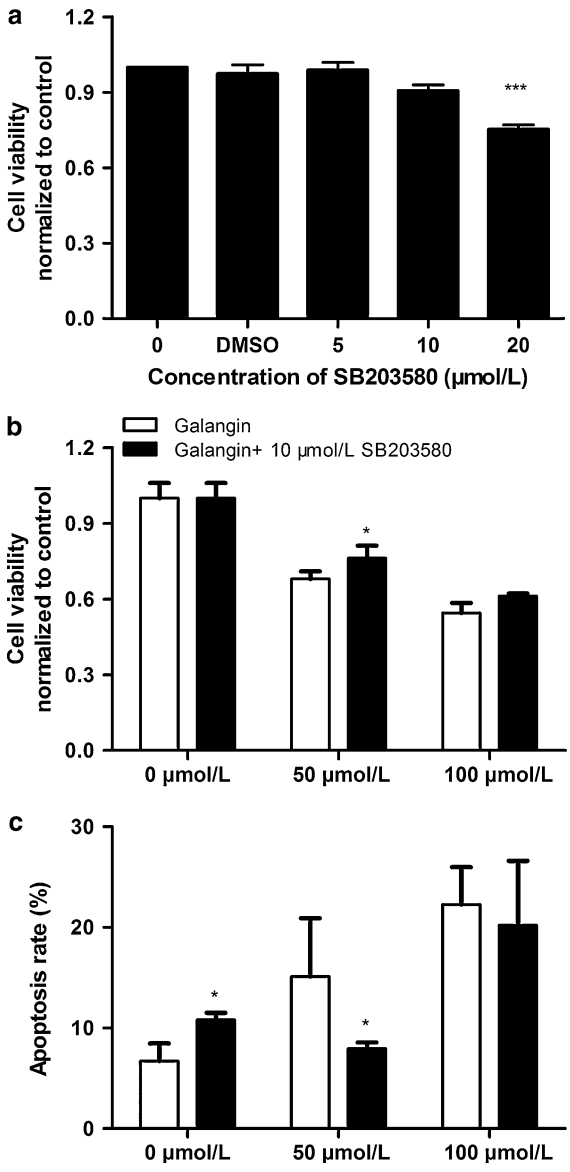

Fig. 5 Effects of SB203580 alone or in combination with galangin on cell viability and apoptosis in B16F10 cells. B16F10 cells were treated with a concentrations of SB203580 as indicated in figure **a** and effects of SB203580 on galangin-induced cytotoxicity in B16F10 cells are shown **b**, B16F10 cells were treated with a galangin (0, 50, and 100 μmol/L) alone or in combination with 10 μmol/L SB203580 for 24 h. Cell viability was determined by the PrestoBlue™ assay. ***$p < 0.001$ versus control group, *$p < 0.05$ statistically different from 50 μmol/L galangin alone and with SB203580. **c** Effects of SB203580 on galangin-induced apoptosis in B16F10 cells. *$p < 0.05$. Data shown represent mean ± SEM, Three independent experiments were performed

resveratrol showed that activation of the p38 MAPK pathway was required for inducing apoptosis in malignant B cells (Shimizu et al. 2006). Jun et al. also indicated that overproduction of reactive oxygen species by bupivaine resulted in dissipation of mitochondrial membrane potential of SH-SY5Y cells, leading to p38 MAPK activation (Lu et al. 2011). Little information is available concerning the functional role of p38 MAPK in galangin-induced cytotoxicity, particularly in malignant melanoma cells. To elucidate the precise mechanism implicated in the galangin-induced cell apoptosis, the effects of galangin on p38 MAPK were examined in B16F10 cells. Concentration titration indicated that galangin activated the phosphorylation of p38 MAPK in a dose dependent manner during apoptosis. Moreover, the sustained activation of p38 MAPK in a time dependent manner from 2 to 24 h was also evident. SB203580, an inhibitor of p38, partially restored galangin-induced apoptosis in B16F10 cells. These results revealed that sustained activation of p38 MAPK is one of the contributors, but not the main one, in galangin-induced apoptosis.

Taken together, we may speculate that galangin suppressed B16F10 melanoma cells proliferation and induced apoptosis via the mitochondrial pathway. And sustained activation of p38 MAPK was implicated in galangin-induced apoptosis. These results provide a novel insight into the molecular mechanisms of galangin and suggest that it may be a promising anti-melanoma therapeutic agent.

Acknowledgments This study was supported, in part, by the Science and Technology Development Fund of the Macao Special Administrative Region (071/2009/A3 and 091/2009/A), the National Key Basic Research Project from Chinese Ministry of Science and Technology (2012CB967004), the Chinese National Nature Sciences Foundation (81121062, 50973046, 31070706), the Jiangsu Provincial Nature Science Foundation (BK2010046, BZ2010074, BZ2011048, BK2011228), Bureau of Science and Technology of Changzhou (CN20100016, CZ20100008, CE20115034, CZ20110028).

References

Atallah E, Flaherty L (2005) Treatment of metastatic malignant melanoma. Curr Treat Options Oncol 6:185–193

Barbarić M, Mišković K, Bojić M, Lončar MB, Smolčić-Bubalo A, Debeljak Z, Medić-Šarić M (2011) Chemical composition of the ethanolic propolis extracts and its effect on HeLa cells. J Ethnopharmacol 135:772–778

Bestwick CS, Milne L (2006) Influence of galangin on HL-60 cell proliferation and survival. Cancer Lett 243:80–89

Chen Y, Bathula SR, Yang Q, Huang L (2010) Targeted nanoparticles deliver siRNA to melanoma. J Invest Dermatol 130:2790–2798

Cohen GM (1997) Caspases: the executioners of apoptosis. Biochem J 326:1–16

Gomez-Lazaro M, Galindo MF, de Melero-Fernandez Mera RM, Fernandez-Gómez FJ, Concannon CG, Segura MF, Comella JX, Prehn JH, Jordan J (2007) Reactive oxygen species and p38 mitogen-activated protein kinase activate Bax to induce mitochondrial cytochrome c release and apoptosis in response to malonate. Mol Pharmacol 71: 736–743

Han J, Sun P (2007) The pathways to tumor suppression via route p38. Trends Biochem Sci 32:364–371

Heo MY, Jae LH, Jung SS, Au WW (1996) Anticlastogenic effects of galangin against mitomycin C-induced micronuclei in reticulocytes of mice. Mutat Res 360:37–41

Heo MY, Sohn SJ, Au WW (2001) Anti-genotoxicity of galangin as a cancer chemopreventive agent candidate. Mutat Res 488:135–150

Kajiya K, Ichiba M, Kuwabara M, Kumazawa S, Nakayama T (2001) Role of lipophilicity and hydrogen peroxide formation in the cytotoxicity of flavonols. Biosci Biotechnol Biochem 65:1227–1229

Kennedy NJ, Davis RJ (2003) Role of JNK in tumor development. Cell Cycle 2:199–201

Kim JD, Liu L, Guo W, Meydani M (2006) Chemical structure of flavonols in relation to modulation of angiogenesis and immune-endothelial cell adhesion. J Nutr Biochem 17: 165–176

Lavrik IN, Golks A, Krammer PH (2005) Caspases: pharmacological manipulation of cell death. J Clin Invest 115: 2665–2672

Lopez-Bergami P (2011) The role of mitogen- and stress-activated protein kinase pathways in melanoma. Pigment Cell Melanoma Res 24:902–921

Lu YH, Lin T, Wang ZT, Wei DZ, Xiang HB (2007) Mechanism and inhibitory effect of galangin and its flavonoid mixture from Alpinia officinarum on mushroom tyrosinase and B16 murine melanoma cells. J Enzyme Inhib Med Chem 22: 433–438

Lu J, Xu SY, Zhang QG, Xu R, Lei HY (2011) Bupivacaine induces apoptosis via mitochondria and p38 MAPK dependent pathways. Eur J Pharmacol 657:51–58

Matsuda H, Nakashima S, Oda Y, Nakamura S, Yoshikawa M (2009) Melanogenesis inhibitors from the rhizomes of Alpinia officinarum in B16 melanoma cells. Bioorg Med Chem 17:6048–6053

Murray TJ, Yang X, Sherr DH (2006) Growth of a human mammary tumor cell line is blocked by galangin, a naturally occurring bioflavonoid, and is accompanied by down-regulation of cyclins D3, E, and A. Breast Cancer Res 8:R17

Olson JM, Hallahan AR (2004) p38 MAP kinase: a convergence point in cancer therapy. Trends Mol Med 10:125–129

Ratheesh A, Ingle A, Gude RP (2007) Pentoxifylline modulates cell surface integrin expression and integrin mediated adhesion of B16F10 cells to extracellular matrix components. Cancer Biol Ther 6:1743–1752

Russo A, Longo R, Vanella A (2002) Antioxidant activity of propolis: role of caffeic acid phenethyl ester and galangin. Fitoterapia 73:S21–S29

Sakamuru S, Li X, Attene-Ramos MS, Huang R, Lu J, Shou L, Shen M, Tice RR, Austin CP, Xia M (2012) Application of a homogenous membrane potential assay to assess mitochondrial function. Physiol Genomics 44:495–503

Shimizu T, Nakazato T, Xian MJ, Sagawa M, Ikeda Y, Kizaki M (2006) Resveratrol induces apoptosis of human malignant B cells by activation of caspase-3 and p38 MAP kinase pathways. Biochem Pharmacol 71:742–750

Sohn SJ, Huh IH, Au WW, Heo MY (1998) Antigenotoxicity of galangin against *N*-methyl-*N*-nitrosourea. Mutat Res 402: 231–236

Szliszka E, Czuba ZP, Bronikowska J, Mertas A, Paradysz A, Krol W (2011) Ethanolic extract of propolis augments TRAIL-induced apoptotic death in prostate cancer cells. Evid Based Complement Alternat Med 2011:535172

Tan Y, Yu R, Pezzuto JM (2003) Betulinic acid-induced programmed cell death in human melanoma cells involves mitogen-activated protein kinase activation. Clin Cancer Res 9:2866–2875

Wang ZJ, Zhang Q, Zhao XH (2009) Suppressive effect of galangin on human esophageal squamous cell carcinoma cell line KYSE-510. Chin J Biochem Mol Biol 25:563–569

Zhang HT, Luo H, Wu J, Lan LB, Fan DH, Zhu KD, Chen XY, Wen M, Liu HM (2010) Galangin induces apoptosis of hepatocellular carcinoma cells via the mitochondrial pathway. World J Gastroenterol 16:3377–3384